



Space-deployable device based on shape memory cyanate ester composites

Chengjun Zeng^a, Liwu Liu^a, Yang Du^b, Miao Yu^b, Xiaozhou Xin^a, Peilei Xu^a, Fengfeng Li^a,
Linlin Wang^c, Fenghua Zhang^c, Yanju Liu^{a,**}, Jinsong Leng^{c,*}

^a Department of Astronautical Science and Mechanics, Harbin Institute of Technology (HIT), P.O. Box 301, No. 92 West Dazhi Street, Harbin, 150001, People's Republic of China

^b Shanghai Institute of Satellite Engineering, No. 3666 Yuanjiang Street, Shanghai, 201109, People's Republic of China

^c Center for Composite Materials and Structures, Harbin Institute of Technology (HIT), P.O. Box 3011, No. 2 YiKuang Street, Harbin, 150080, People's Republic of China

ARTICLE INFO

Keywords:

Cyanate ester
Shape memory polymer composites
Space-deployable structures
Thermomechanical properties

ABSTRACT

Shape memory cyanate ester is a class of shape memory polymers with high thermal stability and excellent space environmental adaptability. In this study, a space-deployable device based on cyanate ester-based shape memory polymer composite (CE-SMPC) was proposed, and its thermomechanical properties and shape memory behavior were experimentally evaluated. The space-deployable device maintained a high shape fixity rate even after prolonged exposure to high or low temperatures, which ensured its locking reliability in space applications. The results of self-deployment experiments indicated that the space-deployable device exhibited good shape recovery performance in both atmospheric and vacuum environments. The SMPC-based space-deployable device presented in this study was applied to China's first Mars exploration mission to achieve autonomous locking and release of the deployable engineering measurement subsystem on the probe.

1. Introduction

As typical representatives of stimulus-responsive materials, shape memory polymers (SMPs) possess the ability to retain a temporary shape and revert to their original shape in response to thermal, optical, electrical, magnetic, or other stimuli [1,2]. SMPs have the advantages of large deformability, low density, and adjustable transition temperature, but poor mechanical properties and recovery force hinder their engineering applications [3,4]. By doping reinforcing fillers into SMPs, the mechanical properties of SMPs can be substantially enhanced without weakening the shape memory properties [5]. Some micro- and nanomaterials tend to exhibit good magnetic conductivity, electrical conductivity, or photothermal effects, so doping these micro- and nanomaterials may impart magnetic, electrical, or optical driving properties to SMPs [6,7].

In some deformable structures with high requirements for mechanical properties, continuous fibers or fiber fabrics are more advantageous than micro- and nanomaterials [8,9]. For example, Li et al. [10] fabricated unidirectional fiber-reinforced shape memory polymer composites (SMPCs) with different fiber contents. Herath et al. [11] prepared fiber fabric-reinforced epoxy-based SMPCs and investigated the

thermomechanical properties and shape memory behavior of SMPCs. Overcoming the shortcomings of SMPs such as low modulus/strength and low recovery force, SMPCs have been widely used as functional and structural materials in aerospace, medical devices and intelligent robots [12]. In the aerospace field, SMPCs are expected to replace traditional smart materials such as shape memory alloys for various space-deployable structures and locking-release mechanisms due to their low density and large deformability [13]. Zhang et al. [14] designed an ultra-lightweight SMPC-based locking-release mechanism for locking and deploying operations of CubeSats' solar arrays. Liu et al. [15] assembled multiple SMPC hinges to a solar array to achieve its controlled deployment. Several space-deployable structures based on SMPCs have passed proof-of-principle and have achieved preliminary applications in spacecraft [16,17]. For example, an SMPC substrate completed deployment experiments and radiation resistance validation in geosynchronous satellite orbit [16]. Recently, the application of epoxy-based SMPC in the Mars Exploration Project was first reported [18].

Despite these advances, most of the applications of SMPCs in space-deployable structures are focused on epoxy-based SMPCs. Compared with epoxy-based SMPCs, cyanate ester-based SMPCs (CE-SMPCs) have

* Corresponding author.

** Corresponding author.

E-mail addresses: yj_liu@hit.edu.cn (Y. Liu), lengjs@hit.edu.cn (J. Leng).

<https://doi.org/10.1016/j.coco.2023.101690>

Received 4 May 2023; Received in revised form 15 July 2023; Accepted 4 August 2023

Available online 5 August 2023

2452-2139/© 2023 Elsevier Ltd. All rights reserved.

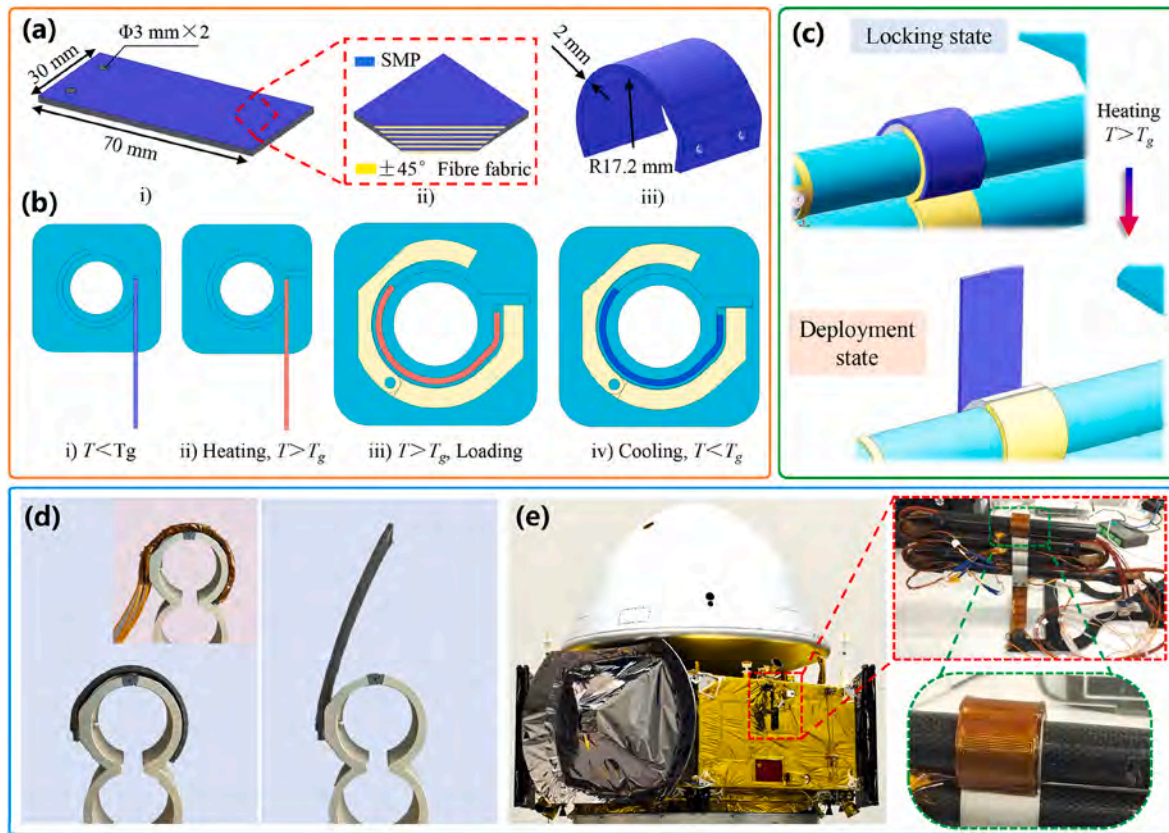


Fig. 1. Design of the space-deployable device. (a) Original and temporary shapes of CE-SMPC laminate. (b) The shape programming process of CE-SMPC laminate. (c) Two operating states of the space-deployable device based on CE-SMPC laminates. (d) Physical diagram of the space-deployable device. (e) The space-deployable device was applied to the Tianwen-1 probe.

more stable thermodynamic properties, better resistance to space irradiation, and higher glass transition temperature (T_g) [19]. In this study, space-deployable devices based on CE-SMPCs were proposed, and systematic experimental characterizations were carried out to verify the thermomechanical reliability of the devices. Finally, the space-deployable device was applied to China's Tianwen-1 Mars probe.

2. Materials and methods

2.1. Structural design

The key component of the space-deployable device is an SMPC laminate with an original rectangular shape (Fig. 1a). SMPC laminate consists of cyanate-based SMP and carbon fiber fabric. Based on the shape memory effect of SMP, the SMPC laminate was programmed into a circular shape at a temperature above the T_g of SMPC and a fixed temporary shape was obtained by cooling (Fig. 1b). The SMPC laminate was used as a space-deployable device in the deployable engineering measurement subsystem on the Tianwen-1 Mars probe. As shown in Fig. 1c, the SMPC laminate with a curved temporary shape locks the two aluminum alloy blocks in the deployable engineering measurement subsystem. After heating the SMPC laminate to a temperature above T_g , the SMPC laminate is transformed from a curved to rectangular shape, and the two alloy blocks are released and deployed.

2.2. Materials and fabrication

The raw materials used to manufacture SMPC laminates are shape memory cyanate ester and carbon fiber fabric (Plain, 3K, 200 g m⁻²) purchased from TORAY, Japan. Shape memory cyanate ester was synthesized by adding bis (hydroxy)-terminated and bis(epoxy)-terminated

polyethers (Rm-OH and Rn-CH₂CH₂O, Sigma-Aldrich (Shanghai) Trading Co., Ltd.) to bisphenol A cyanate monomer (BACEM, Jiangsu Wujiao Resin Factory, China) [20]. BACEM was melted in a beaker at 120 °C. Then the modifiers Rm-OH and Rn-CH₂CH₂O were added into BACEM and stirred continuously for 30 minutes to obtain a homogeneous pre-polymerized solution. CE-SMPC laminates were fabricated by a vacuum-assisted resin transfer molding process, and the mass fraction of the fiber was about 50%. The six-layer carbon fiber fabrics were first laid in a rigid mold wrapped in a vacuum bag, and then the cyanate pre-polymerized solution was injected into the vacuum bag by a vacuum pump. CE-SMPC laminates were obtained after being cured at 150 °C for 2 hours, 180 °C for 2 hours, and 210 °C for 3 hours. The heating rate was 0.25 °C/min⁻¹.

A 230-type film electric heater (Beijing Hongyu Space Technology Co., Ltd.) with a resistance value of 28 Ω was attached to the CE-SMPC laminate. Double-sided pressure-sensitive tape acted as a binder between the laminate and the film heater, and 3 M 92# polyimide film tape was used to wrap the laminate. Fig. 1d shows the images of the CE-SMPC laminate before and after deployment. The space-deployable device based on the CE-SMPC laminate was applied in the Tianwen-1 probe (Fig. 1e) [21], before which it was subjected to three deformation-recovery operations.

2.3. Characterization methods

The surface morphology of CE-SMPC was characterized by the digital light microscope (VHX-900, Keyence, Japan). Fourier transform infrared (FTIR) spectroscopy analysis of CE-SMPC samples was performed using the FTIR spectrometer (Thermo Scientific Nicolet iS50). Thermogravimetric analysis (TGA) was carried out by a thermogravimetric analyzer (NETZSCH TG 209) from 25 °C to 800 °C at 10 °C/min. Dynamic

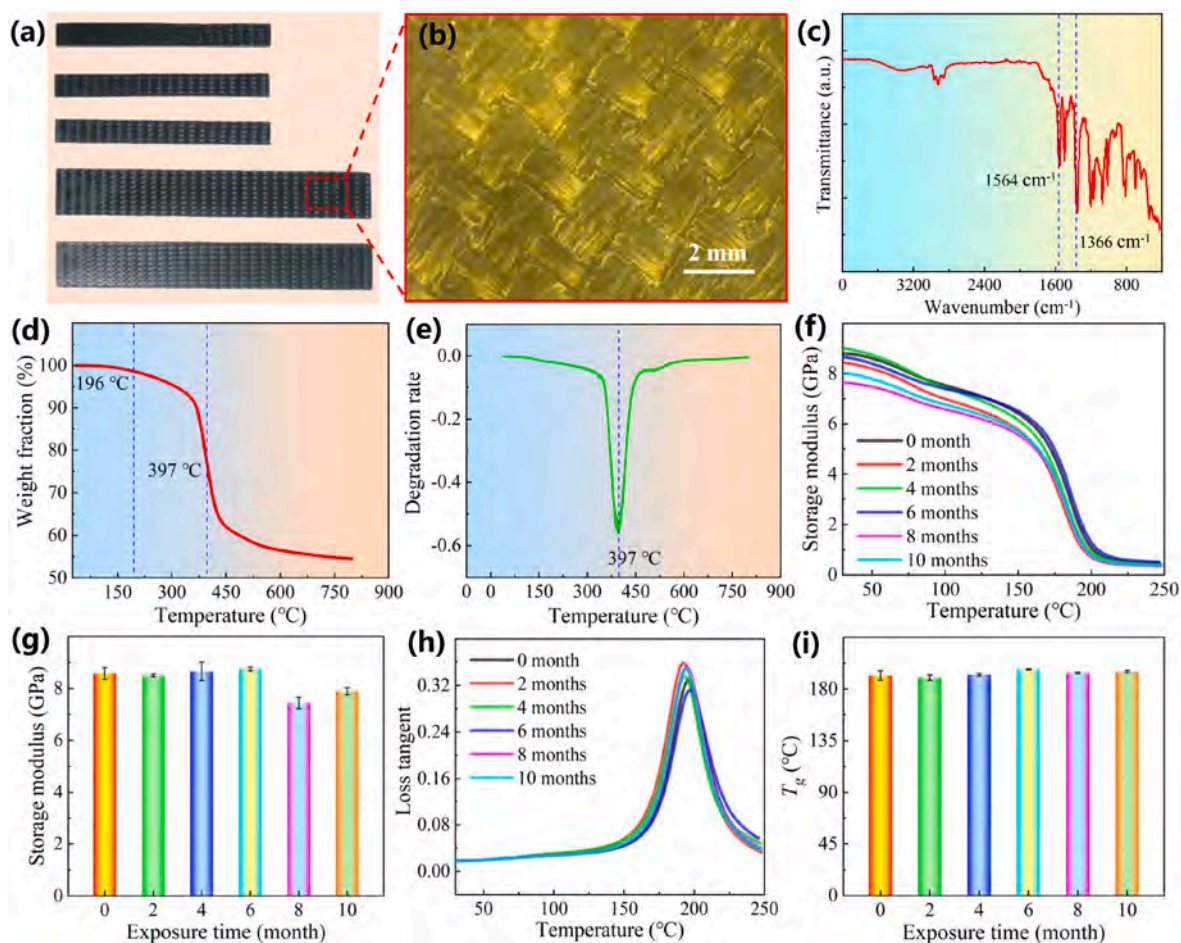


Fig. 2. Thermomechanical properties of CE-SMPC. (a) CE-SMPC samples. (b) Surface micromorphology of the sample. (c) FTIR spectrum. (d) Thermogravimetric curve. (e) DTG curve. (f) Storage modulus curves of CE-SMPC after exposure to low temperature. (g) Effect of exposure time at low temperature on the storage modulus. (h) Loss tangent curves of CE-SMPC after exposure to low temperature. (i) Effect of exposure time at low temperature on the T_g .

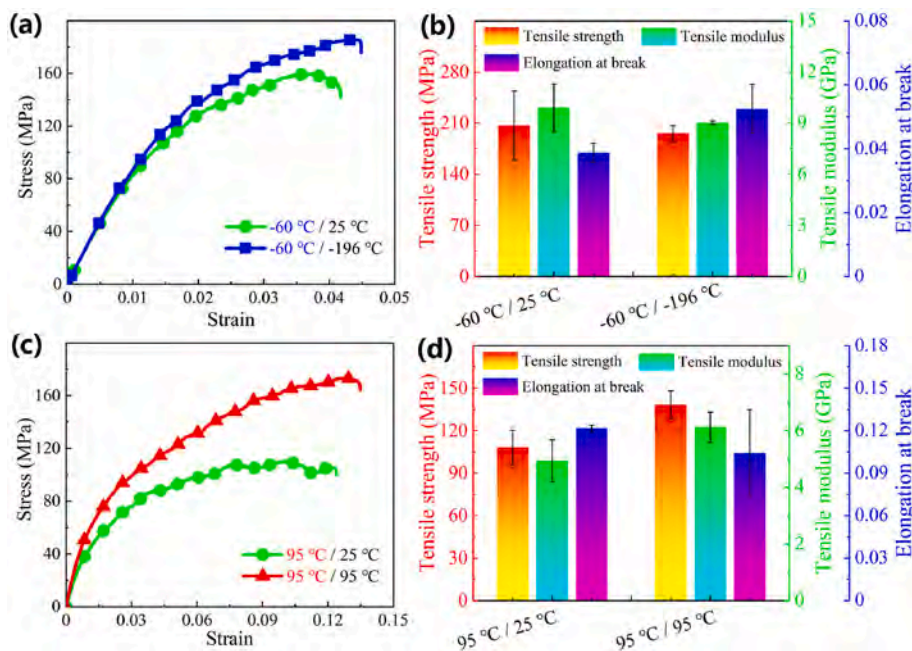


Fig. 3. Effect of high or low-temperature exposure on the tensile properties of CE-SMPC. (a) Tensile stress-strain curves and (b) tensile properties at low temperature ($-65\text{ }^{\circ}\text{C}$) after long-term RT or low-temperature exposure. (c) Tensile stress-strain curves and (d) tensile properties at high temperature ($95\text{ }^{\circ}\text{C}$) after long-term RT or high-temperature exposure.

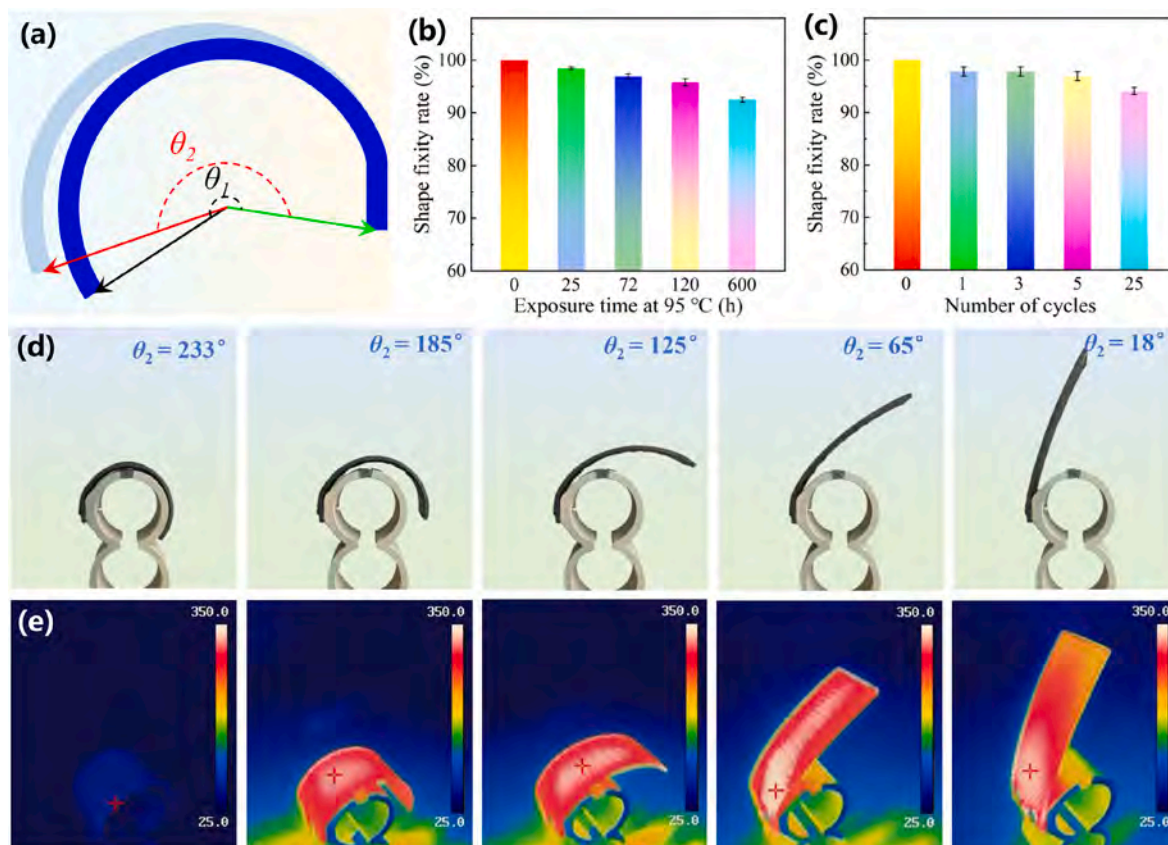


Fig. 4. Self-deployment performance of the space-deployable device in the atmospheric environment. (a) Schematic diagram of the recovery angle. (b) Effect of high-temperature exposure on shape fixity rate. (c) Effect of high and low-temperature cycling on shape fixity rate. (d) Self-deployment process of the space-deployable device in the atmospheric environment. (e) Temperature distribution clouds of the space-deployable device during self-deployment.

mechanical analysis (DMA) of samples exposed to liquid nitrogen ($-196\text{ }^{\circ}\text{C}$) for various times (0–10 months) was accomplished through a Dynamic Mechanical Analyzer (DMA Q800) with a loading frequency of 1 Hz.

According to ASTM standard D3039/D3039 M, uniaxial tensile tests of CE-SMPC samples exposed to different temperatures ($-196\text{ }^{\circ}\text{C}$, $25\text{ }^{\circ}\text{C}$ or $95\text{ }^{\circ}\text{C}$) for 1 month were carried out by the MTS 809 axial/torsion test system, and two test temperatures were selected, namely $-60\text{ }^{\circ}\text{C}$ and $95\text{ }^{\circ}\text{C}$. Self-deployment experiments of the space-deployable device based on CE-SMPC laminates were conducted under both atmospheric pressure and vacuum (pressure below 10^{-3} Pa). Self-deployment experiments in the vacuum tank were carried out utilizing electrical heating. A heating power of 30 W was applied to the device, and the local temperature change in the device was monitored by a thermistor.

3. Results and discussion

3.1. Thermomechanical properties of CE-SMPC

The reinforcing phase in CE-SMPC is carbon fiber plain fabric in which the warp and weft yarns are distributed at $\pm 45^{\circ}$ (Fig. 2a and b). Compared with unidirectional fibers, fiber fabrics not only enhance the transverse/longitudinal mechanical properties of CE-SMPC but also improve the shear resistance and fracture toughness of CE-SMPC. FTIR spectroscopy was used to analyze the characteristic functional groups of the cyanate ester resin. In the FTIR curve of CE-SMPC, the characteristic peaks at 1366 cm^{-1} and 1564 cm^{-1} were stretching vibrational absorption peaks of 1,3,5-triazine groups, which indicated that the carbon-nitrogen triple bond ($-\text{CN}$) of the cyanate group in the cyanate monomer undergoes self-polymerization (Fig. 2c) [20]. The thermal stability of

CE-SMPC was evaluated by TGA. Fig. 2d presents the TGA curve of CE-SMPC, and the corresponding derivative thermogravimetry (DTG) curve is shown in Fig. 2e, which reflects the rate of change in the mass of the sample with temperature. The temperature corresponding to the maximum decomposition rate is $397\text{ }^{\circ}\text{C}$, and the high thermal decomposition temperature indicates that CE-SMPC possesses satisfactory heat resistance.

The storage modulus curves of CE-SMPC after experiencing cryogenic exposure are given in Fig. 2f. The variable stiffness capability of CE-SMPC was not affected after ten months of exposure to liquid nitrogen. No visible change in the initial storage modulus ($30\text{ }^{\circ}\text{C}$) occurred during the first six months of cryogenic exposure. After eight months of cryogenic exposure, the storage modulus decreased but was still higher than 7 Gpa (Fig. 2g), indicating that CE-SMPC still exhibited excellent load-bearing capacity after long-term cryogenic exposure. As seen from the loss tangent curves, long-term cryogenic exposure did not affect the T_g of CE-SMPC, which was always maintained around $196\text{ }^{\circ}\text{C}$ (Fig. 2h and i).

CE-SMPC often experiences complex high or low-temperature environments in various engineering applications, so it makes sense to explore the mechanical properties of CE-SMPC after prolonged exposure to high or low temperatures. The tensile responses of CE-SMPC at $-60\text{ }^{\circ}\text{C}$ after one month of exposure to room temperature (RT, $25\text{ }^{\circ}\text{C}$) or low temperature ($-196\text{ }^{\circ}\text{C}$, liquid nitrogen environment) are given in Fig. 3a and b. Cryogenic exposure slightly weakened the tensile modulus and strength of CE-SMPC but enhanced the elongation at break. The tensile properties of CE-SMPC at $95\text{ }^{\circ}\text{C}$ after one month of exposure to RT or high temperature ($95\text{ }^{\circ}\text{C}$) are presented in Fig. 3c and d. High-temperature exposure effectively improved the tensile strength and modulus of CE-SMPC, which was attributed to the increase in crosslink

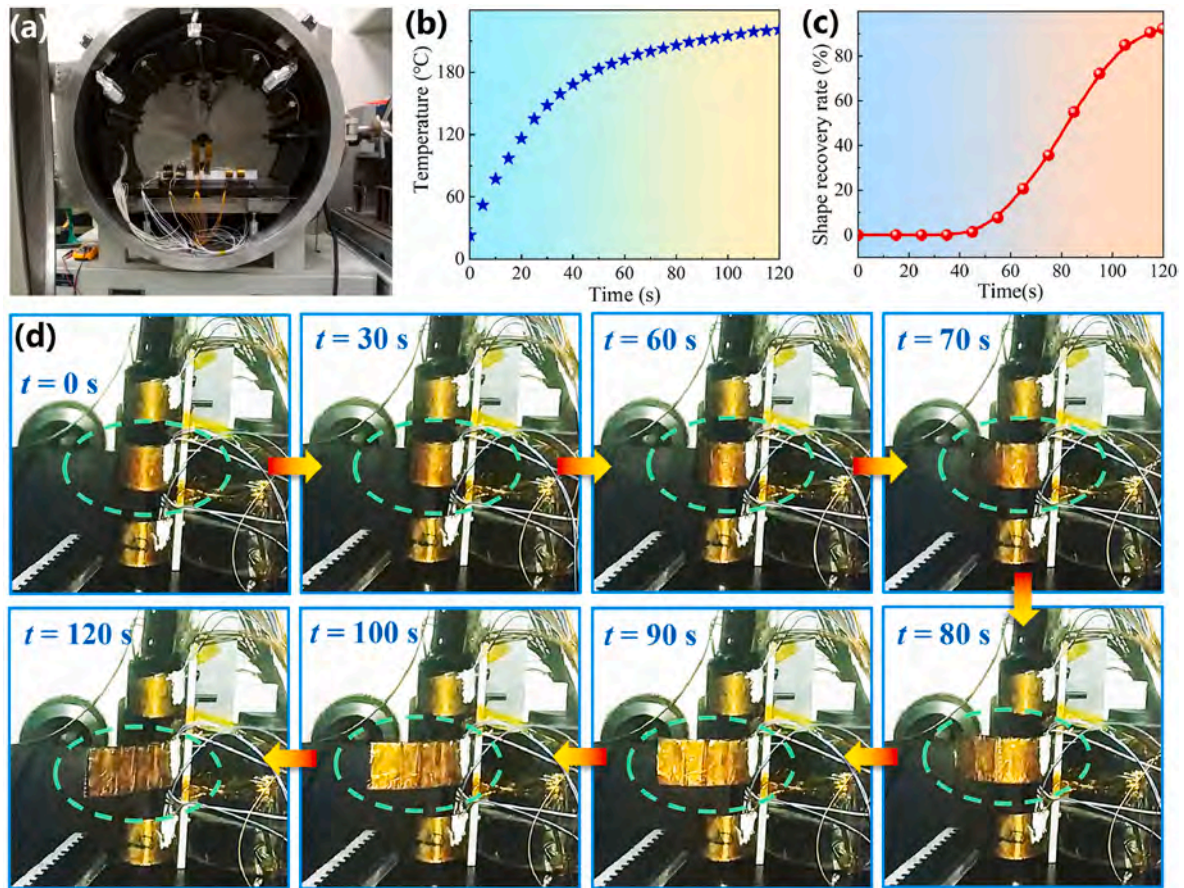


Fig. 5. Self-deployment performance of the space-deployable device in the vacuum environment. (a) Equipment for thermal vacuum experiments. (b) Evolution of the local temperature in the device with the power-on time. (c) Evolution of shape recovery rate with the power-on time. (d) The deployment process of the space-deployable device in the vacuum environment.

density of the cyanate ester due to its post-curing in the high-temperature environment.

3.2. Functional validation of space-deployable device

CE-SMPC is a viscoelastic composite, so the effect of temperature and time on the shape fixity ability of CE-SMPC needs to be studied to evaluate the long-term locking function of the space-deployable device. As shown in Fig. 4a, the initial central angle of the curved device is θ_1 and the central angle after experiencing long-term storage is θ_2 , so the shape fixity rate is defined as $Shape\ fixity\ rate = \theta_2 / \theta_1 \times 100\%$.

Fig. 4b presents the shape fixity rate of the device after exposure to high temperature (95 °C) for different times, from which it is found that the shape fixity rate gradually decreases as the exposure time increases. Notably, the shape fixity rate eventually converges to a stable value. Fig. 4c gives the shape fixity rate of the space-deployable device after undergoing thermal cycling. Each cycle lasted 24 hours, with 12 hours of exposure at 95 °C and 12 hours at -196 °C. After 25 thermal cycles, the shape fixity rate of the device approached an equilibrium of 92.5%.

To verify the unlocking and deployment functions of the space-deployable device, the shape recovery experiments were executed in atmospheric and vacuum environments, respectively. The shape recovery process of the device in the atmospheric environment is shown in Fig. 4d, and the maximum shape recovery rate is 92%, where the shape recovery rate is defined as $Shape\ recovery\ rate = (\theta_1 - \theta_2) / \theta_1 \times 100\%$. The device was heated locally by a heat gun, and the temperature distribution cloud in the device during the heating process is presented in Fig. 4e. A uniform temperature distribution in the device was observed.

The thermal vacuum deployment experiment of the space-

deployable device was performed in a thermal vacuum tank (Fig. 5a). The temperature in the device gradually converged to the equilibrium value of 220 °C with the power-on time (Fig. 5b). Fig. 5c depicts the shape recovery rate versus power-on time. The shape of the device was not changed during the first 60 s of heating because the temperature in the device had not yet reached the T_g of CE-SMPC. Rapid shape recovery was observed as the temperature reached the T_g of CE-SMPC. Fig. 5d illustrates the thermal vacuum shape recovery process of the space-deployable device, where the shape of the device remains stable after heating for 120 s.

4. Conclusions

A space-deployable device based on CE-SMPC was designed and validated for China's Tianwen-1 Mars exploration mission. FTIR analysis, TGA, DMA and mechanical tests were carried out to characterize the molecular structure and thermomechanical properties of CE-SMPC. The test results demonstrated that CE-SMPC possessed high thermal stability and mechanical properties. After high or low-temperature exposure, the space-deployable device maintained a high shape fixity rate, which ensured high locking reliability in space applications. Self-deployment experiments of the device in atmospheric and vacuum environments were conducted, and the results confirmed that it can be effectively deployed in both ground and space environments. The space-deployable device based on CE-SMPC presented in this study was applied to the Tianwen-1 Mars probe, enabling the autonomous locking and release of the deployable engineering measurement subsystem on the probe [21].

CRedit authorship contribution statement

Chengjun Zeng: Methodology, Investigation, Visualization, Writing – original draft. **Liwu Liu:** Investigation, Formal analysis. **Yang Du:** Methodology, Formal analysis. **Miao Yu:** Investigation, Visualization. **Xiaozhou Xin:** Methodology, Experiment. **Peilei Xu:** Data curation, Experiment. **Fengfeng Li:** Funding acquisition, Writing – review & editing. **Linlin Wang:** Investigation, Experiment. **Fenghua Zhang:** Data curation, Conceptualization. **Yanju Liu:** Supervision, Writing – review & editing. **Jinsong Leng:** Supervision, Project administration.

Declaration of competing interest

We declare that we do not have any commercial or associative interest that represents a conflict of interest in connection with the work submitted.

Data availability

No data was used for the research described in the article.

Acknowledgment

This work is supported by the National Natural Science Foundation of China (Grant No. 12102107).

References

- [1] S. Yang, Y. He, J. Leng, Shape memory poly (ether ether ketone)s with tunable chain stiffness, mechanical strength and high transition temperatures, *Int. J. Smart Nano Mater.* 13 (2022) 1–16.
- [2] J. Meurer, R.H. Kampes, T. Bätz, J. Hniopek, O. Müschke, J. Kimmig, S. Zechel, M. Schmitt, J. Popp, M.D. Hager, U.S. Schubert, 3D-Printable shape-memory polymers based on halogen bond interactions, *Adv. Funct. Mater.* 32 (2022), 2207313.
- [3] D. Kyeong, M. Kim, M. Kwak, Thermally triggered multilevel diffractive optical elements tailored by shape-memory polymers for temperature history sensors, *ACS Appl. Mater. Interfaces* 15 (2023), 9813–9819.
- [4] X. Xin, L. Liu, Y. Liu, J. Leng, Prediction of effective thermomechanical behavior of shape memory polymer composite with micro-damage interface, *Compos. Commun.* 25 (2021), 100727.
- [5] M. Amini, S. Wu, Designing a polymer blend nanocomposite with triple shape memory effects, *Compos. Commun.* 23 (2021), 100564.
- [6] J. Gu, X. Zhang, H. Duan, M. Wan, H. Sun, A hygro-thermo-mechanical constitutive model for shape memory polymers filled with nano-carbon powder, *Int. J. Smart Nano Mater.* 12 (2021) 286–306.
- [7] R.E. Booth, C. Khanna, H.M. Schrickx, S. Siddika, A. Al Shafe, B.T. O'Connor, Electrothermally actuated semitransparent shape memory polymer composite with application as a wearable touch sensor, *ACS Appl. Mater. Interfaces* 14 (2022) 53129–53138.
- [8] A. Asar, M.S. Irfan, K.A. Khan, W. Zaki, R. Umer, Self-sensing shape memory polymer composites reinforced with functional textiles, *Compos. Sci. Technol.* 221 (2022), 109219.
- [9] Y. Li, X. Chen, J. Zhou, X. Liu, D. Zhang, F. Du, W. He, P. Jia, H. Liu, A review of high-velocity impact on fiber-reinforced textile composites: potential for aero engine applications, *Int. J. Mech. Syst. Dyn.* 2 (2022) 50–64.
- [10] F. Li, F. Scarpa, X. Lan, L. Liu, Y. Liu, J. Leng, Bending shape recovery of unidirectional carbon fiber reinforced epoxy-based shape memory polymer composites, *Compos. Part A-Appl. Sci. Manuf.* 116 (2019) 169–179.
- [11] H.M.C.M. Herath, J.A. Epaarachchi, M.M. Islam, W. Al-Azzawi, J. Leng, F. Zhang, Structural performance and photothermal recovery of carbon fibre reinforced shape memory polymer, *Compos. Sci. Technol.* 167 (2018) 206–214.
- [12] Y. Zhang, T. Liu, X. Lan, Y. Liu, J. Leng, L. Liu, A compliant robotic grip structure based on shape memory polymer composite, *Compos. Commun.* 36 (2022), 101383.
- [13] L. Xie, Y. Wang, G. Chen, H. Feng, N. Zheng, H. Ren, Q. Zhao, T. Xie, A thermadaptable epoxy based on borate ester crosslinking and its carbon fiber composite as rapidly processable prepreg, *Compos. Commun.* 28 (2021), 100979.
- [14] D. Zhang, L. Liu, J. Leng, Y. Liu, Ultra-light release device integrated with screen-printed heaters for CubeSat's deployable solar arrays, *Compos. Struct.* 232 (2020), 111561.
- [15] Z. Liu, X. Lan, W. Bian, L. Liu, Q. Li, Y. Liu, J. Leng, Design, material properties and performances of a smart hinge based on shape memory polymer composites, *Compos. Part B-Eng.* 193 (2020), 108056.
- [16] F. Li, L. Liu, X. Lan, C. Pan, Y. Liu, J. Leng, Q. Xie, Ground and geostationary orbital qualification of a sunlight-stimulated substrate based on shape memory polymer composite, *Smart Mater. Struct.* 28 (2019), 075023.
- [17] X. Lan, L. Liu, F. Zhang, Z. Liu, L. Wang, Q. Li, F. Peng, S. Hao, W. Dai, X. Wan, Y. Tang, M. Wang, Y. Hao, Y. Yang, C. Yang, Y. Liu, J. Leng, World's first spaceflight on-orbit demonstration of a flexible solar array system based on shape memory polymer composites, *Sci. China Technol. Sci.* 63 (2020) 1436–1451.
- [18] D. Zhang, L. Liu, P. Xu, Y. Zhao, Q. Li, X. Lan, F. Zhang, L. Wang, X. Wan, X. Zou, C. Zeng, X. Xin, W. Dai, Y. Li, Y. He, Y. Liu, J. Leng, World's first application of a self-deployable mechanism based on shape memory polymer composites in Mars explorations: ground-based validation and on-Mars qualification, *Smart Mater. Struct.* 31 (2022), 115008.
- [19] L. Wang, F. Zhang, Y. Liu, S. Du, J. Leng, Thermal, mechanical and shape fixity behaviors of shape memory cyanate under γ -ray radiation, *Smart Mater. Struct.* 31 (2022), 045010.
- [20] L. Wang, F. Zhang, Y. Liu, J. Leng, γ -rays radiation resistant shape memory cyanate ester resin and its composites with high transition temperature, *Smart Mater. Struct.* 28 (2019), 075039.
- [21] C. Zeng, L. Liu, Y. Du, M. Yu, X. Xin, T. Liu, P. Xu, Y. Yan, D. Zhang, W. Dai, X. Lan, F. Zhang, L. Wang, X. Wan, W. Bian, Y. Liu, J. Leng, A Shape-Memory Deployable Subsystem with a Large Folding Ratio in China's Tianwen-1 Mars Exploration Mission, 2023. *Engineering*.